

# Pyrolysis of propane under vacuum carburizing conditions: An experimental and modeling study

R.U. Khan <sup>a,\*</sup>, S. Bajohr <sup>a</sup>, D. Buchholz <sup>a</sup>, R. Reimert <sup>a</sup>, H.D. Minh <sup>b</sup>,  
K. Norinaga <sup>b</sup>, V.M. Janardhanan <sup>b</sup>, S. Tischer <sup>b</sup>, O. Deutschmann <sup>b</sup>

<sup>a</sup> Engler-Bunte-Institut, Bereich Gas, Erdöl und Kohle, Engler Bunte Ring 1, Universität Karlsruhe, 76131 Karlsruhe, Germany

<sup>b</sup> Institute of Chemical Technology, University of Karlsruhe, 76128 Karlsruhe, Germany

Received 2 March 2007; accepted 7 September 2007

Available online 12 October 2007

## Abstract

Propane has been pyrolyzed in a flow reactor system at different temperatures ranging from 640 °C to 1010 °C and at 8 mbar of partial pressure which are typical vacuum carburizing conditions for steel. Nitrogen was used as a carrier gas. The products of pyrolysis were collected and analyzed by gas chromatography. The reactor was numerically simulated by 1D and 2D flow models coupled to a detailed gas phase reaction mechanism. The gas atmosphere composition has been predicted under the conditions of vacuum carburizing of steel.

© 2007 Elsevier B.V. All rights reserved.

**Keywords:** Propane; Pyrolysis; Modeling; Simulation; Carburizing

## 1. Introduction

Propane is a widely used feedstock in the petrochemical industry and hence much effort has been devoted to the study of the kinetics of its pyrolysis at varying conditions. Pyrolysis of propane like that of many other hydrocarbons leads to hundreds of species and reactions. The reaction mechanisms proposed in the literature range from few species to hundreds of species [1–10]. The experimental conditions reported also vary over a wide range of temperatures, residence times and pressures depending upon their field of application.

With the development of computational chemistry, detailed kinetic mechanisms based on elementary reactions can be used to predict the gas phase composition. The usability of such mechanisms for simulations of different reactors is more easy and systematic.

The description of the gas phase composition during hydrocarbon pyrolysis is important in many engineering applications including vacuum gas carburizing of steel. During vacuum gas carburizing, steel parts are normally exposed to a carburizing gas such as propane or acetylene at temperatures of

approximately 950 °C and total pressure between 2 and 20 mbar. Under the high temperature, the carburizing gas is pyrolyzed and forms atomic carbon on the steel surface. The carbon diffuses into the steel surface and locally increases the carbon concentration resulting in increased hardness of steel after an appropriate heat treatment. The pyrolysis of carburizing gas also results in the formation of higher hydrocarbons, soot, and pyrocarbon which settle on the furnace walls causing operational problems [11–15].

There are several control techniques available for the conventional gas carburizing at atmospheric pressure which allow to control the carbide layers and overall control of the process. But in the case of low-pressure or vacuum carburizing, such techniques can not be used due to the absence of thermodynamic equilibrium [16]. However there are some efforts to develop such techniques but not frequently available at commercial scale [17]. The experimental data or models describing the behaviour of the gas atmosphere for vacuum carburizing are not at least frequently available from the literature. In the present work, the pyrolysis of propane was studied at different temperatures ranging from 690 °C to 1010 °C at a partial pressure of 8 mbar which are typical vacuum carburizing conditions of steel. Aim of modeling was to predict the gas atmosphere composition under particular experimental conditions with computational tools and available

\* Corresponding author.

E-mail address: [rafi\\_ullah.khan@ciw.uni-karlsruhe.de](mailto:rafi_ullah.khan@ciw.uni-karlsruhe.de) (R.U. Khan).

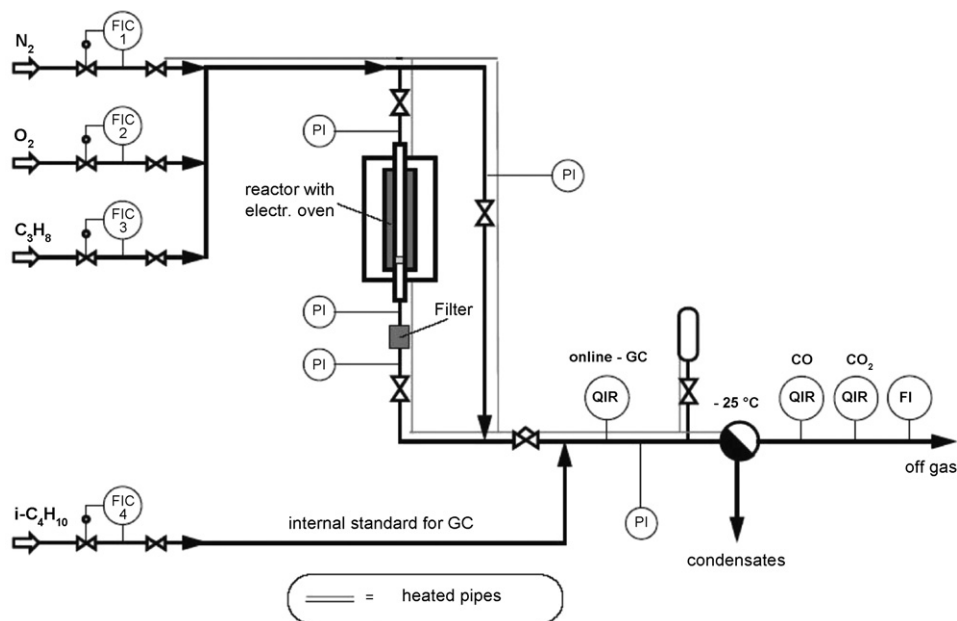


Fig. 1. Flow sheet of the laboratory scale apparatus used for the experimental investigation.

detailed mechanisms. Consequently, 1D and 2D flow field descriptions and a detailed mechanism based on elementary reactions implemented in the software package DETCHEM [18] were used to simulate the reactor behavior.

## 2. Experimental

The laboratory scale apparatus used for the experiments in the presented paper consists of the gas feed system, the reactor and the product gas analysis as shown in Fig. 1. The gas feed system consists of four mass flow equivalents (Brooks Model 5850) for propane ( $C_3H_8$ ),  $N_2$ ,  $O_2$  and *iso*-butane ( $i-C_4H_{10}$ ). Nitrogen is used as an inert carrier gas,  $O_2$  for burning the deposited carbon from pyrolysis and *iso*-butane as internal standard for gas chromatography as it is only formed in negligible amounts during the propane pyrolysis under the investigated reaction conditions. There is also a facility to bypass the reactor and analyze the inlet gas composition for calibration purposes. The reactor shown in Fig. 2 consists of an alumina ( $Al_2O_3$ ) pipe with an inner diameter of 20 mm, outer diameter of 25 mm and a length of 600 mm. An alumina ( $Al_2O_3$ ) filter is placed at the outlet of the reactor to separate any possibly formed solid carbon from the gas stream. The temperature profile was measured at the center of the reactor as shown in Fig. 2 by a NiCr/Ni thermocouple in 6 mm i.d. alumina ( $Al_2O_3$ ) pipe. Gas chromatography was performed on two gas chromatographs. The gaseous products  $C_3H_8$ ,  $CH_4$ ,  $C_2H_2$ ,  $C_2H_4$ ,  $C_2H_6$ , and  $C_3H_6$  were measured by Hewlett-Packard GC Type 5890 equipped with a  $30\text{ m} \times 0.53\text{ mm}$  i.d. methylsiloxane capillary column ( $15\text{ }\mu\text{m}$  film thickness). The higher hydrocarbons ( $C_{5+}$ ) were measured by Hewlett-Packard GC Type 5890 equipped with a  $50\text{ m} \times 0.2\text{ mm}$  i.d. methylsiloxane capillary column ( $0.5\text{ }\mu\text{m}$  film thickness) which can separate hydrocarbons containing up to 30 carbon atoms. The GC system was calibrated by determining a carbon response

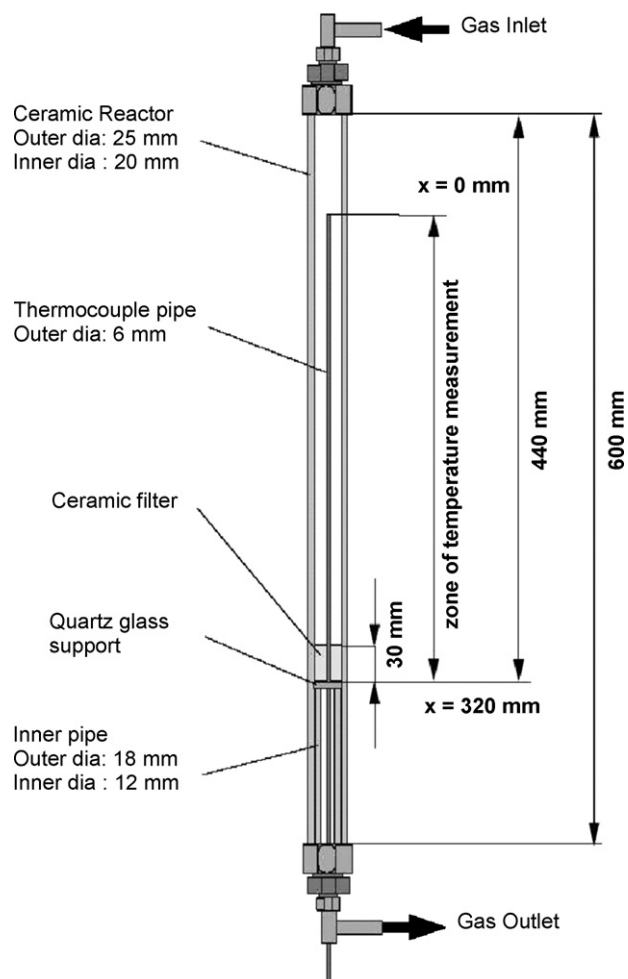


Fig. 2. Sketch of the reactor used for the experimental investigations.

factor for the product hydrocarbons using *iso*-butane. Hydrogen, not measured in the pyrolysis product stream, was calculated by a hydrogen mass balance not taking into account any traces of H<sub>2</sub> eventually bound in the deposited carbon. The carbon deposited was burned with a mixture of 5 vol.% O<sub>2</sub> in N<sub>2</sub>. Both CO and CO<sub>2</sub> formed by burning the deposited carbon were analysed by an infrared analyser and were used for the carbon balancing.

### 3. Modeling approaches

#### 3.1. One-dimensional model

Simulations were carried out by using PLUG module of DETCHEM 2.0 with a detailed kinetic mechanism [10]. Plug-flow equations enormously reduce the computational cost by simplifying the balance equations for mass, species and energy. These equations are derived based on the assumptions of (a) negligible axial diffusion and (b) infinite mixing in the radial direction. Assumption (b) means that there is no variation in the transverse direction. Furthermore, DETCHEM<sup>PLUG</sup> is a steady-state model. Hence, the 1D partial differential conservation equations become ordinary differential equations with the axial coordinate as time-like variable.

With these assumption, the system of differential-algebraic equations (DAE) consist of the continuity equation

$$A_c \frac{d(\rho u)}{dz} = 0, \quad (1)$$

the equation for conservation of the  $k$ -th species ( $k = 1, \dots, k_g$ )

$$A_c \frac{d(\rho u Y_k)}{dz} = M_k A_c \dot{\omega}_k, \quad (2)$$

the energy equation

$$\rho u A_c \frac{d(c_p T)}{dz} + \sum_{k=1}^{k_g} \dot{\omega}_k h_k M_k A_c = U A_s (T_w - T), \quad (3)$$

and the ideal gas law is assumed as equation of state

$$p \bar{M} = \rho R T. \quad (4)$$

In these equations  $\rho$  is the density,  $u$  the velocity,  $A_c$  the area of cross section,  $A_s$  the surface area per unit length,  $k_g$  the number of gas phase species,  $\dot{\omega}_k$  the molar rate of production or removal of species  $k$  by gas-phase reactions,  $M_k$  the molecular mass of the species  $k$ ,  $Y_k$  the mass fraction of species  $k$ ,  $c_p$  the specific heat capacity,  $h_k$  the specific enthalpy of the species  $k$ ,  $U$  the overall heat transfer coefficient,  $T$  the gas temperature,  $T_w$  the wall temperature,  $p$  the pressure, and  $\bar{M}$  is the average molecular weight.

The DAE system is integrated using the solver LIMEX. The input consists of kinetic parameters for reactions in the Arrhenius format and thermodynamic data as polynomial fits in temperature.

#### 3.2. Two-dimensional model

DETCHEM<sup>CHANNEL</sup> was used for these simulations with the same mechanism as for the 1D simulations. This program solves a parabolic system of differential-algebraic equations, which are obtained by simplifying the Navier–Stokes equations using the same assumptions as in the boundary-layer approximation. That is, since there is a preferred direction of transport due to convection along the axis of a channel, the diffusive transport in axial direction is neglected. However, in radial direction both convective and diffusive transports are considered, but radial pressure gradients vanish.

The CHANNEL model solves the following steady-state equations in cylinder symmetric form:

- continuity equation

$$\frac{\partial \rho u}{\partial z} + \frac{1}{r} \frac{\partial (r \rho v)}{\partial r} = 0, \quad (5)$$

- conservation of axial momentum

$$\rho u \frac{\partial u}{\partial z} + \rho v \frac{\partial u}{\partial r} = -\frac{\partial p}{\partial z} + \frac{1}{r} \frac{\partial}{\partial r} \left( \mu r \frac{\partial u}{\partial r} \right), \quad (6)$$

- conservation of radial momentum (radial pressure gradients vanish)

$$0 = \frac{\partial p}{\partial r}, \quad (7)$$

- conservation of species  $k$  ( $k = 1, \dots, k_g$ )

$$\rho u \frac{\partial Y_k}{\partial z} + \rho v \frac{\partial Y_k}{\partial r} = -\frac{1}{r} \frac{\partial (r J_{k,r})}{\partial r} + \dot{\omega}_k M_k, \quad (8)$$

- conservation of thermal energy

$$\rho c_p \left( u \frac{\partial T}{\partial z} + v \frac{\partial T}{\partial r} \right) = \frac{1}{r} \frac{\partial}{\partial r} \left( r \lambda \frac{\partial T}{\partial r} \right) - \sum_{k=1}^{k_g} c_{pk} J_{k,r} \frac{\partial T}{\partial r} - \sum_{k=1}^{k_g} h_k \dot{\omega}_k M_k. \quad (9)$$

Here, in addition  $r$  is the radial coordinate,  $v$  the radial velocity,  $\mu$  the viscosity,  $\lambda$  the thermal conductivity, and  $J_{k,r}$  is the radial component of the mass flux vector.

Again, ideal gas law (Eq. (4)) is used as equation of state. In steady state, we require a vanishing mass flux at the wall as boundary condition. The temperature at the gas-phase-wall boundary is given as a function of axial position.

We applied a van-Mises transformation to the above equations, which leads to a simplified system of partial differential equations without an explicit appearance of the radial velocity component  $v$ . After that, these equations are semi-discretized with respect to the transformed radial coordinate by the method of lines. Therefore, the discretized grid in radial direction is non-uniform. The resulting system of differential-algebraic equations (DAE) is solved by an implicit method, based on the backward differentiation formulas (BDF), with variable order, variable step size control methods and an efficient modified Newton method for the solution of the nonlinear equations arising from the BDF discretization [19].

Table 1

Consumption and formation of major species at 870 °C, 0.8 s and 8 mbar partial pressure of propane

Consumption of C <sub>3</sub> H <sub>8</sub>		Formation of C <sub>3</sub> H <sub>8</sub>	
C <sub>2</sub> H <sub>5</sub> + CH <sub>3</sub> = C <sub>3</sub> H <sub>8</sub>	32%	C <sub>2</sub> H <sub>3</sub> + I - C <sub>3</sub> H <sub>7</sub> = C <sub>2</sub> H <sub>2</sub> + C <sub>3</sub> H <sub>8</sub>	12%
C <sub>3</sub> H <sub>8</sub> + CH <sub>3</sub> = N - C <sub>3</sub> H <sub>7</sub> + CH <sub>4</sub>	5%	C <sub>2</sub> H <sub>5</sub> + I - C <sub>3</sub> H <sub>7</sub> = C <sub>2</sub> H <sub>4</sub> + C <sub>3</sub> H <sub>8</sub>	41%
C <sub>3</sub> H <sub>8</sub> + CH <sub>3</sub> = I - C <sub>3</sub> H <sub>7</sub> + CH <sub>4</sub>	4%	AC <sub>3</sub> H <sub>5</sub> + I - C <sub>3</sub> H <sub>7</sub> = AC <sub>3</sub> H <sub>4</sub> + C <sub>3</sub> H <sub>8</sub>	41%
C <sub>3</sub> H <sub>8</sub> + H = N - C <sub>3</sub> H <sub>7</sub> + H <sub>2</sub>	27%	I - C <sub>3</sub> H <sub>7</sub> + I - C <sub>3</sub> H <sub>7</sub> = C <sub>3</sub> H <sub>6</sub> + C <sub>3</sub> H <sub>8</sub>	2%
C <sub>3</sub> H <sub>8</sub> + H = I - C <sub>3</sub> H <sub>7</sub> + H <sub>2</sub>	27%		
C <sub>3</sub> H <sub>8</sub> + C <sub>2</sub> H <sub>5</sub> = I - C <sub>3</sub> H <sub>7</sub> + C <sub>2</sub> H <sub>6</sub>	3%	Consumption of CH <sub>4</sub>	
Formation of CH <sub>4</sub>		CH <sub>4</sub> + C <sub>6</sub> H <sub>5</sub> = C <sub>6</sub> H <sub>6</sub> + CH <sub>3</sub>	99%
H + CH <sub>3</sub> + M = CH <sub>4</sub> + M	1%		
H <sub>2</sub> + CH <sub>3</sub> = CH <sub>4</sub> + H	40%		
H <sub>2</sub> + C <sub>2</sub> H <sub>5</sub> = CH <sub>4</sub> + CH <sub>3</sub>	2%		
C <sub>2</sub> H <sub>4</sub> + CH <sub>3</sub> = CH <sub>4</sub> + C <sub>2</sub> H <sub>3</sub>	16%		
CH <sub>3</sub> + C <sub>2</sub> H <sub>6</sub> = CH <sub>4</sub> + C <sub>2</sub> H <sub>5</sub>	9%		
C <sub>3</sub> H <sub>6</sub> + CH <sub>3</sub> = CH <sub>4</sub> + AC <sub>3</sub> H <sub>5</sub>	2%		
CH <sub>3</sub> + C <sub>3</sub> H <sub>8</sub> = CH <sub>4</sub> + N - C <sub>3</sub> H <sub>7</sub>	11%		
CH <sub>3</sub> + C <sub>3</sub> H <sub>8</sub> = CH <sub>4</sub> + I - C <sub>3</sub> H <sub>7</sub>	10%		
Formation of C <sub>2</sub> H <sub>2</sub>		Consumption of C <sub>2</sub> H <sub>2</sub>	
C <sub>2</sub> H <sub>3</sub> + M = C <sub>2</sub> H <sub>2</sub> + H + M	75%	C <sub>2</sub> H <sub>2</sub> + AC <sub>3</sub> H <sub>5</sub> = L - C <sub>5</sub> H <sub>7</sub>	1%
SC <sub>3</sub> H <sub>5</sub> = C <sub>2</sub> H <sub>2</sub> + CH <sub>3</sub>	14%	C <sub>2</sub> H <sub>2</sub> + AC <sub>3</sub> H <sub>5</sub> = H + C <sub>5</sub> H <sub>6</sub>	48%
C <sub>3</sub> H <sub>6</sub> = CH <sub>4</sub> + C <sub>2</sub> H <sub>2</sub>	1%	C <sub>2</sub> H <sub>2</sub> + C <sub>5</sub> H <sub>5</sub> = C <sub>7</sub> H <sub>7</sub>	38%
C <sub>4</sub> H <sub>6</sub> = C <sub>2</sub> H <sub>2</sub> + C <sub>2</sub> H <sub>4</sub>	1%	C <sub>2</sub> H <sub>2</sub> + C <sub>7</sub> H <sub>7</sub> = C <sub>9</sub> H <sub>8</sub> + H	10%
Formation of C <sub>2</sub> H <sub>4</sub>		Consumption of C <sub>2</sub> H <sub>4</sub>	
C <sub>2</sub> H <sub>5</sub> + M = C <sub>2</sub> H <sub>4</sub> + H + M	43%	C <sub>2</sub> H <sub>4</sub> + H = H <sub>2</sub> + C <sub>2</sub> H <sub>3</sub>	50%
C <sub>2</sub> H <sub>3</sub> + C <sub>2</sub> H <sub>6</sub> = C <sub>2</sub> H <sub>4</sub> + C <sub>2</sub> H <sub>5</sub>	1%	C <sub>2</sub> H <sub>4</sub> + CH <sub>3</sub> = CH <sub>4</sub> + C <sub>2</sub> H <sub>3</sub>	41%
C <sub>3</sub> H <sub>6</sub> + H = C <sub>2</sub> H <sub>4</sub> + CH <sub>3</sub>	6%	C <sub>2</sub> H <sub>4</sub> + C <sub>2</sub> H <sub>3</sub> = C <sub>4</sub> H <sub>6</sub> + H	4%
N - C <sub>3</sub> H <sub>7</sub> = C <sub>2</sub> H <sub>4</sub> + CH <sub>3</sub>	42%		
I - C <sub>3</sub> H <sub>7</sub> = C <sub>2</sub> H <sub>4</sub> + CH <sub>3</sub>	6%		
Formation of C <sub>2</sub> H <sub>6</sub>		Consumption of C <sub>2</sub> H <sub>6</sub>	
CH <sub>3</sub> + CH <sub>3</sub> + M = C <sub>2</sub> H <sub>6</sub> + M	87%	H + C <sub>2</sub> H <sub>6</sub> = CH <sub>4</sub> + CH <sub>3</sub>	1%
C <sub>2</sub> H <sub>5</sub> + C <sub>3</sub> H <sub>8</sub> = C <sub>2</sub> H <sub>6</sub> + I - C <sub>3</sub> H <sub>7</sub>	12%	H + C <sub>2</sub> H <sub>6</sub> = H <sub>2</sub> + C <sub>2</sub> H <sub>5</sub>	71%
		CH <sub>3</sub> + C <sub>2</sub> H <sub>6</sub> = CH <sub>4</sub> + C <sub>2</sub> H <sub>5</sub>	21%
		C <sub>2</sub> H <sub>3</sub> + C <sub>2</sub> H <sub>6</sub> = C <sub>2</sub> H <sub>4</sub> + C <sub>2</sub> H <sub>5</sub>	5%
Formation of C <sub>3</sub> H <sub>6</sub>		Consumption of C <sub>3</sub> H <sub>6</sub>	
CH <sub>3</sub> + C <sub>2</sub> H <sub>3</sub> = C <sub>3</sub> H <sub>6</sub>	4%	C <sub>3</sub> H <sub>6</sub> + H = C <sub>2</sub> H <sub>4</sub> + CH <sub>3</sub>	43%
H + AC <sub>3</sub> H <sub>5</sub> = C <sub>3</sub> H <sub>6</sub>	8%	C <sub>3</sub> H <sub>6</sub> + H = H <sub>2</sub> + AC <sub>3</sub> H <sub>5</sub>	40%
I - C <sub>3</sub> H <sub>7</sub> + M = C <sub>3</sub> H <sub>6</sub> + H + M	81%	C <sub>3</sub> H <sub>6</sub> + H = H <sub>2</sub> + SC <sub>3</sub> H <sub>5</sub>	1%
N - C <sub>3</sub> H <sub>7</sub> = C <sub>3</sub> H <sub>6</sub> + H	3%	C <sub>3</sub> H <sub>6</sub> + CH <sub>3</sub> = CH <sub>4</sub> + AC <sub>3</sub> H <sub>5</sub>	8%
		C <sub>3</sub> H <sub>6</sub> + CH <sub>3</sub> = CH <sub>4</sub> + SC <sub>3</sub> H <sub>5</sub>	1%
Formation of C <sub>6</sub> H <sub>6</sub>		Consumption of C <sub>6</sub> H <sub>6</sub>	
AC <sub>3</sub> H <sub>4</sub> + C <sub>3</sub> H <sub>3</sub> = C <sub>6</sub> H <sub>6</sub> + H	9%	C <sub>6</sub> H <sub>6</sub> + C <sub>6</sub> H <sub>5</sub> = P <sub>2</sub> + H	9%
C <sub>3</sub> H <sub>3</sub> + AC <sub>3</sub> H <sub>5</sub> = C <sub>6</sub> H <sub>6</sub> + H + H	54%	C <sub>6</sub> H <sub>6</sub> + C <sub>7</sub> H <sub>7</sub> = H + BENZYL <sub>B</sub>	90%
C <sub>2</sub> H <sub>2</sub> + N - C <sub>4</sub> H <sub>5</sub> = C <sub>6</sub> H <sub>6</sub> + H	1%		
H <sub>2</sub> + C <sub>6</sub> H <sub>5</sub> = C <sub>6</sub> H <sub>6</sub> + H	4%		
AlC <sub>2</sub> H <sub>3</sub> + H = C <sub>6</sub> H <sub>6</sub> + C <sub>2</sub> H <sub>3</sub>	2%		
C <sub>2</sub> H <sub>6</sub> + C <sub>6</sub> H <sub>5</sub> = C <sub>6</sub> H <sub>6</sub> + C <sub>2</sub> H <sub>5</sub>	2%		
C <sub>6</sub> H <sub>8</sub> <sub>13</sub> = H <sub>2</sub> + C <sub>6</sub> H <sub>6</sub>	2%		
C <sub>7</sub> H <sub>8</sub> + H = C <sub>6</sub> H <sub>6</sub> + CH <sub>3</sub>	16%		
Formation of H <sub>2</sub>		Consumption of H <sub>2</sub>	
H <sub>2</sub> + C <sub>2</sub> H <sub>3</sub> = C <sub>2</sub> H <sub>4</sub> + H	10%	CH <sub>4</sub> + H = H <sub>2</sub> + CH <sub>3</sub>	94%
H + C <sub>2</sub> H <sub>6</sub> = H <sub>2</sub> + C <sub>2</sub> H <sub>5</sub>	15%	CH <sub>4</sub> + CH <sub>3</sub> = H <sub>2</sub> + C <sub>2</sub> H <sub>5</sub>	5%
C <sub>3</sub> H <sub>6</sub> + H = H <sub>2</sub> + AC <sub>3</sub> H <sub>5</sub>	6%		
H + C <sub>3</sub> H <sub>8</sub> = H <sub>2</sub> + N - C <sub>3</sub> H <sub>7</sub>	29%		
H + C <sub>3</sub> H <sub>8</sub> = H <sub>2</sub> + I - C <sub>3</sub> H <sub>7</sub>	29%		
C <sub>4</sub> H <sub>8</sub> + H = H <sub>2</sub> + N - C <sub>4</sub> H <sub>7</sub>	1%		
H + C <sub>5</sub> H <sub>6</sub> = H <sub>2</sub> + C <sub>5</sub> H <sub>5</sub>	2%		

#### 4. Chemistry of propane pyrolysis

The detailed reaction mechanism consists of 227 species and 827 elementary reactions most of which are reversible. The mechanism was developed for modeling pyrolysis of light hydrocarbons at temperatures of approximately 900 °C. The mechanism and the thermodynamic data for all the

species has already been published [10]. The mechanism does not describe the deposition of solid carbon from the gas phase. The reaction flow analysis was performed by HOMREA software package [20] at 870 °C for 0.8 s residence time. The reactions and their contribution to the consumption or formation of the species of interest are discussed below.

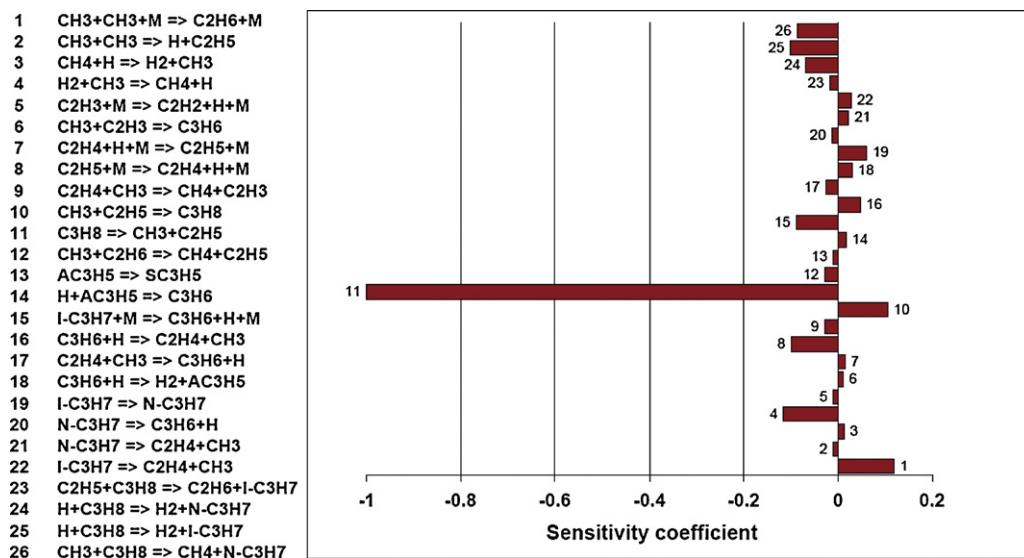


Fig. 3. Sensitivity analysis with respect to propane at 870 °C.

The consumption of propane occurs by six different reactions as shown in Table 1.

The relative importance of these reactions varies with temperature. At the flow reactor and shock tube temperatures these reactions are important with the unimolecular decomposition dominating [21,22]. The sensitivity analysis with respect to propane is also shown in Fig. 3 which reveals the importance of decomposition step of propane resulting in the formation of C<sub>2</sub>H<sub>5</sub> and CH<sub>3</sub> radicals. This step has been recognized as the initiation step in the previous studies [8,21–23]. The first stage in the pyrolysis of propane can be designated as the primary reactions wherein the propane is decomposed through free radical chain mechanism into the principal primary products such as CH<sub>4</sub>, C<sub>2</sub>H<sub>4</sub>, C<sub>3</sub>H<sub>6</sub>, H<sub>2</sub> and other minor primary products. Major source of methane formation is through CH<sub>3</sub> radical while acetylene is formed mainly by the decomposition of C<sub>2</sub>H<sub>3</sub> radical. Ethylene is formed mainly by the decomposition of C<sub>2</sub>H<sub>5</sub> and N-C<sub>3</sub>H<sub>7</sub> radicals while the decomposition of I-C<sub>3</sub>H<sub>7</sub> result in the formation of propylene. Most of the ethane is formed by the recombination of CH<sub>3</sub> radicals. The radical C<sub>3</sub>H<sub>3</sub> reacts with AC<sub>3</sub>H<sub>4</sub> and AC<sub>3</sub>H<sub>5</sub>, respectively, to form 63% of the total benzene formed while 16% of the total benzene is formed by the H radical reaction with toluene. The second stage encompasses secondary

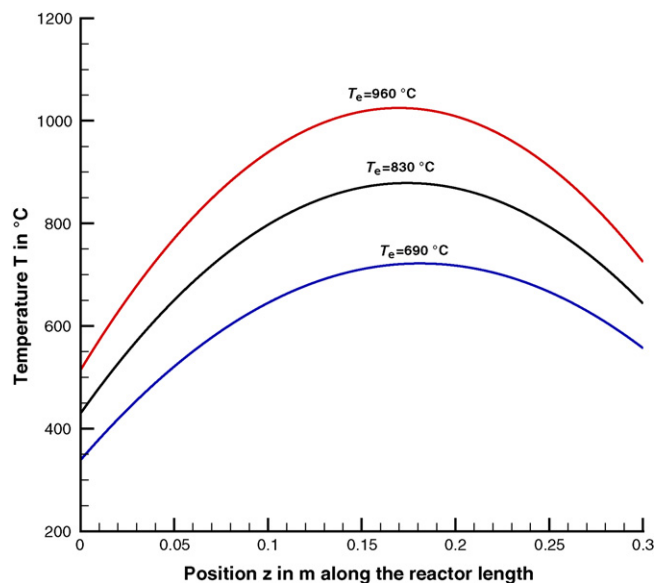
Fig. 4. Temperature profiles for different typical values of equivalent temperature  $T_e$ .

Table 2  
Product distribution in %C based on feed carbon (C1) at various temperatures (experimental)

$T_e$ (°C)	$T_e$ (K)	C <sub>3</sub> H <sub>8</sub>	CH <sub>4</sub>	C <sub>2</sub> H <sub>2</sub>	C <sub>2</sub> H <sub>4</sub>	C <sub>2</sub> H <sub>6</sub>	C <sub>3</sub> H <sub>6</sub>	C <sub>5+</sub>	Soot & Pyr. C
640	913	99.46	0.00	0.00	0.00	0.00	0.27	0.27	0
690	963	94.35	1.70	0.00	0.00	0.00	3.14	0.81	0
730	1003	84.35	2.06	0.00	5.41	0.78	5.24	2.15	0
780	1053	56.20	6.36	0.3	19.75	3.32	10.80	3.14	0.13
830	1103	21.74	11.95	3.11	40.70	5.71	9.55	6.63	0.62
870	1143	3.99	14.93	10.16	50.92	4.57	4.62	8.61	2.22
920	1193	0.00	15.54	19.72	47.96	2.06	1.48	9.41	3.83
960	1233	0.00	15.58	26.29	40.16	0.51	0.54	12.19	4.73
1010	1283	0.00	14.34	38.19	28.06	0.00	0.00	12.28	7.13

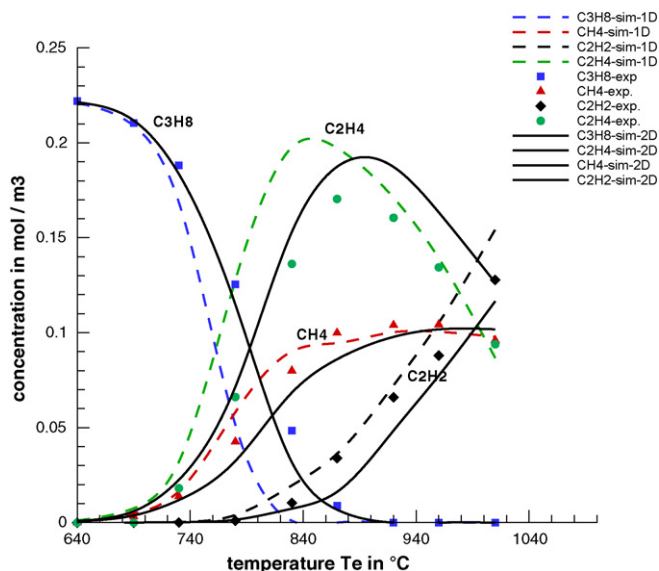


Fig. 5. Comparison of 1D, 2D simulation and experimental results—exit concentrations of smaller hydrocarbons.

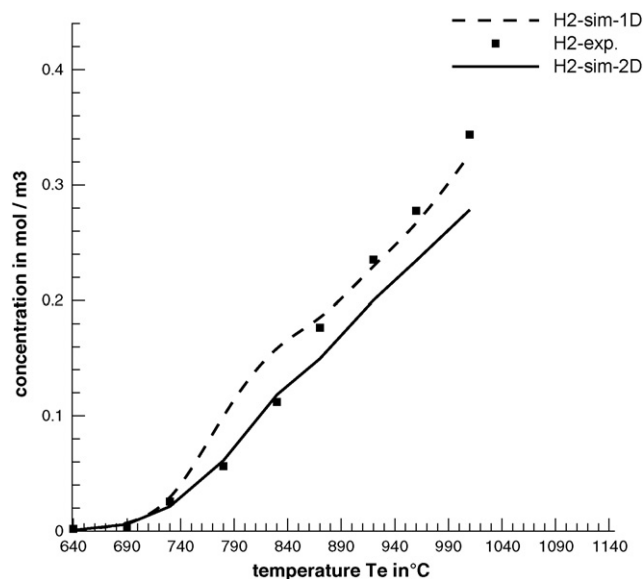


Fig. 8. Comparison of 1D, 2D simulation and experimental results—exit concentrations of hydrogen determined by material balance.

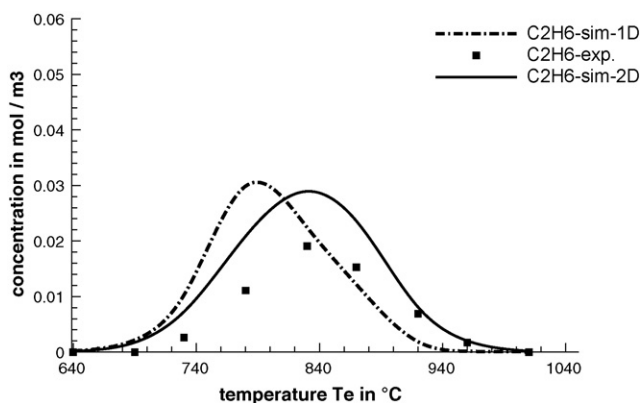


Fig. 6. Comparison of 1D, 2D simulation and experimental results—exit concentrations of  $C_2H_6$ .

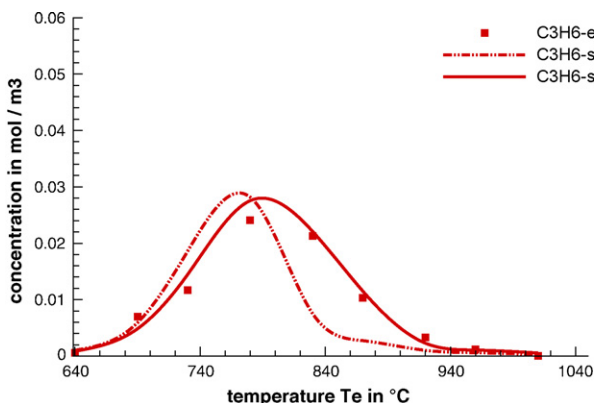


Fig. 7. Comparison of 1D, 2D simulation and experimental results—exit concentrations of  $C_3H_6$ .

reactions involving further pyrolysis of olefins produced by primary reactions, hydrogenation and dehydrogenation reactions of the olefins and condensation reactions wherein two or more smaller fragments combine to produce large stable structures such as cyclodiolefins and aromatics [23,24].

### 5. Results and discussions

The experimentally derived composition as a function of temperature is compared with the results of the 1D and 2D simulations. The partial pressure of propane was kept at 8 mbar for all experiments with the total pressure of 1.6 bar. The inlet flow rate was 150 l/h (NTP) in all the experiments. The

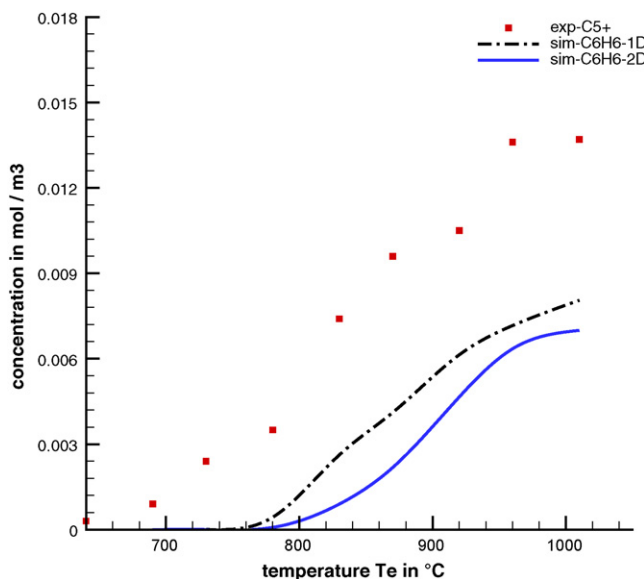


Fig. 9. Comparison of 1D, 2D simulation and experimental results—exit concentrations of higher hydrocarbons ( $C_{5+}$ ).

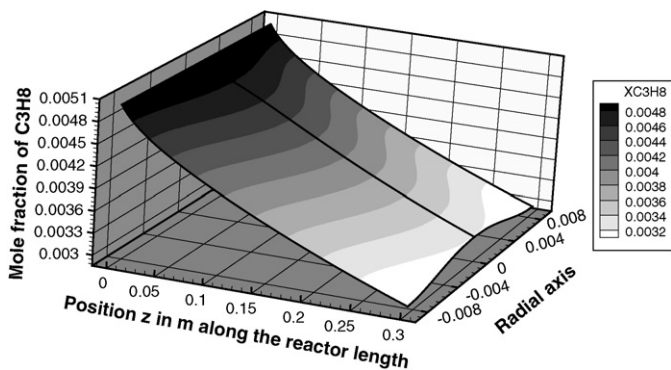


Fig. 10. Propane mole fractions in 2D model at 760 °C.

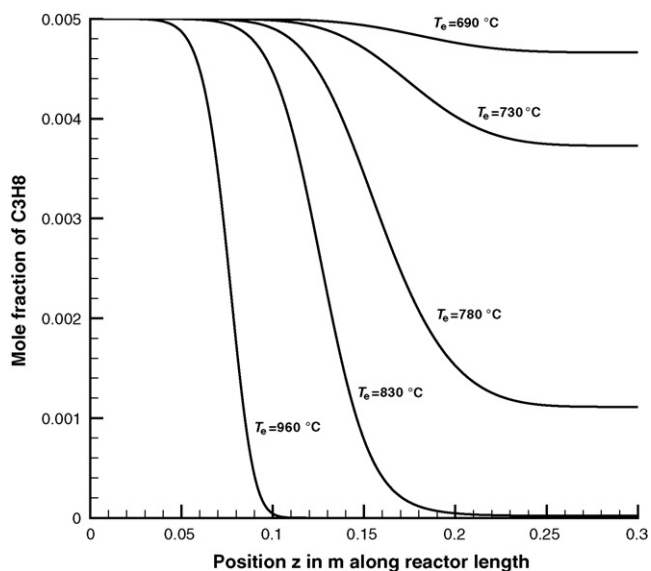


Fig. 11.  $C_3H_8$  mole fraction profiles for 1D model at different values of equivalent temperature  $T_e$  (non-isothermal).

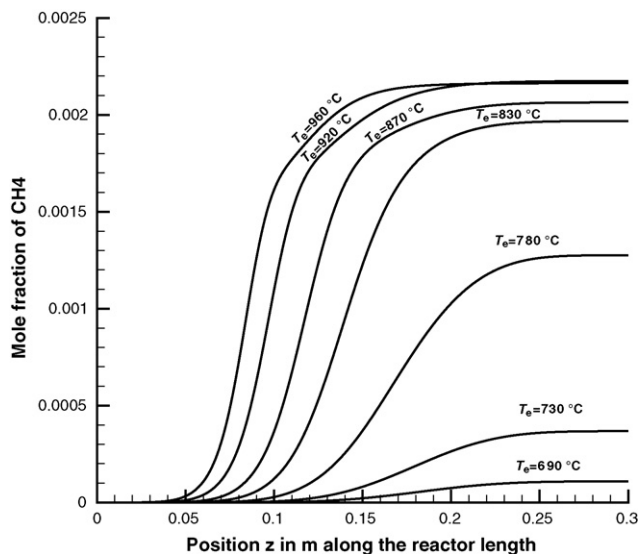


Fig. 12.  $CH_4$  mole fraction profiles for 1D model at different values of equivalent temperature  $T_e$  (non-isothermal).

temperature profile was measured at the center of the reactor and a polynomial fit as shown below was used in the 1D simulations for the description of the temperature field.

$$T(T_e, z) = (az^2 + bz + c)T_e + dz^2 + ez + f \quad (10)$$

where  $T(T_e, z)$  represents the temperature as a function of the position  $z$  along the reactor length, whereas  $T_e$  represents an equivalent temperature and  $a, b, c, d, e$  and  $f$  are the polynomial coefficients with values of  $-0.00223, 0.37, 0.066, -3.20, 0.65$  and  $-110$ , respectively. So the measured temperatures can be computed from the above single equation by substituting the values of given polynomial coefficients and equivalent temperature  $T_e$  at any position  $z$  in centimeters. Typical plots of the temperature profiles for different equivalent temperature values are shown in Fig. 4.

In 2D simulations, the temperature profile was not implemented by the polynomial (10) because it requires wall temperature  $T_w$  as well as gas temperature  $T$ . So the measured inlet gas temperature  $T$  was specified only at the inlet of the reactor while  $T_w$  takes the values according to the measured temperature profile. The temperature profile was divided into small pieces and a piecewise linear temperature profile was implemented by providing two pairs of values of position  $z$  and  $T_w$ .

Table 2 summarizes the gas compositions at various temperatures. The comparisons of the 1D, 2D simulation and experimental results are shown in Figs. 5–9 at various temperatures. In general the agreement between simulation and experimental results is more satisfactory for 2D as compared to 1D simulations (Figs. 5–8). The conversions of propane predicted by the 1D model are slightly higher than the experimental measurements. The deviations can be explained by the differences in the treatment of radial transport limitations of the 1D and 2D models. While the 2D model does not need additional assumptions about the radial transport, the 1D simulation requires empirical models for heat and mass transfer coefficients. Here, the transfer limitations are underestimated. Further, the models implement temperature profiles in a different way as already described. Moreover, the comparison indicates that the reaction mechanism used is suitable to simulate the pyrolysis of propane properly under the given conditions.

A typical parabolic mole fraction profile of propane in 2D is shown in Fig. 10. The hydrocarbons measured as  $C_{5+}$  are compared to the simulation results of  $C_6H_6$  as shown in Fig. 9. The other hydrocarbons, higher than  $C_6H_6$ , present in the model are formed comparatively in small amounts so only the  $C_6H_6$  has been compared to the experimentally measured  $C_{5+}$  hydrocarbons. The difference between simulation and experimental results in this case shows the amount of hydrocarbons other than the  $C_6H_6$  present in the gas phase leading to the soot or solid carbon.

The 2D simulations are more time consuming than 1D simulations. If axial diffusion were included in the model equations, the numerical effort would be even more increased. Nevertheless, the accuracy of the 1D model is sufficient for our

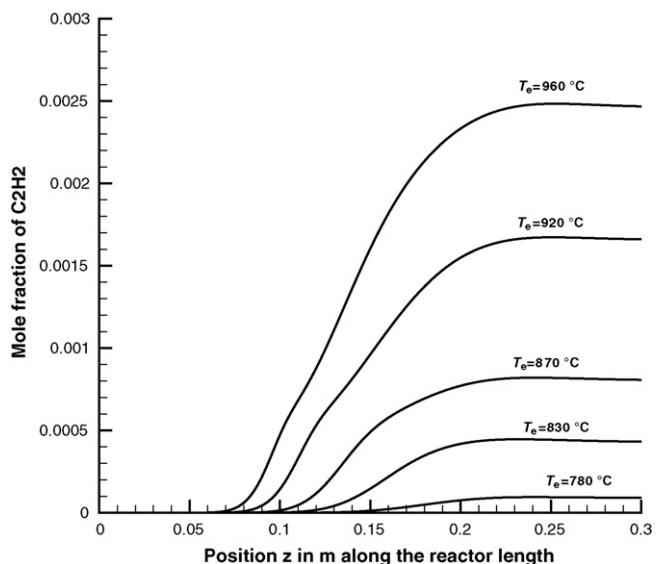


Fig. 13. C<sub>2</sub>H<sub>2</sub> mole fraction profiles for 1D model at different values of equivalent temperature  $T_e$  (non-isothermal).

further discussions, therefore the axial profiles of the 1D simulations only are compared for several temperatures.

Fig. 11 shows the 1D model results for propane at selected temperatures. The decomposition of propane gradually increases with increase of temperature and complete conversion can be achieved only at a fraction of the reactor length at higher temperatures.

Fig. 12 shows 1D model results for CH<sub>4</sub>. The formation of methane is barely affected at temperatures above 850 °C and only a small decrease is observed at temperatures above 950 °C as shown in Fig. 5.

Fig. 13 shows the model predictions for C<sub>2</sub>H<sub>2</sub>. The selectivity for C<sub>2</sub>H<sub>2</sub> gradually increases with temperature.

Fig. 14 shows the mole fraction profiles of C<sub>2</sub>H<sub>4</sub> along the reactor length at various selected temperatures. The maximum

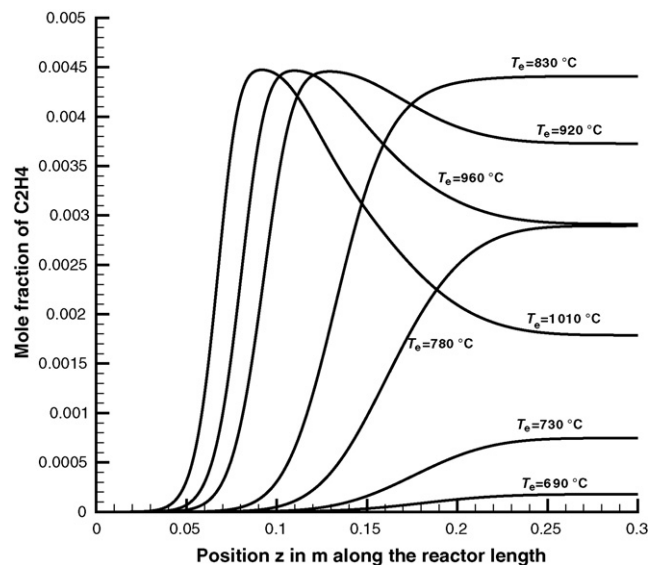


Fig. 14. C<sub>2</sub>H<sub>4</sub> mole fraction profiles for 1D model at different values of equivalent temperature  $T_e$  (non-isothermal).

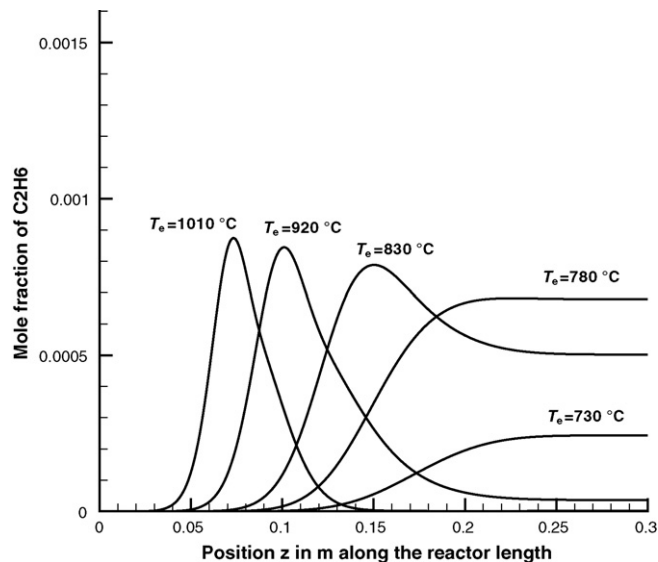


Fig. 15. C<sub>2</sub>H<sub>6</sub> mole fraction profiles for 1D model at different values of equivalent temperature  $T_e$  (non-isothermal).

amount of C<sub>2</sub>H<sub>4</sub> formed shifts toward the reactor inlet at higher values of equivalent temperature  $T_e$ . So the selectivity for C<sub>2</sub>H<sub>4</sub> increases up to a temperature of about 900 °C and then decreases.

The formation of further products of pyrolysis C<sub>3</sub>H<sub>6</sub> and C<sub>2</sub>H<sub>6</sub> is shown in Figs. 15 and 16, respectively. The maximum amount increases up to a temperature of approximately 800 °C and then gradually decreases to very low amounts at higher temperatures.

Fig. 17 shows the mole fractions of H<sub>2</sub> formed at various temperatures. The amount of H<sub>2</sub> formed increases with the increase of temperature.

Thus, the validated model can now be used to study the homogeneous pyrolysis of propane under the technical operating conditions of vacuum carburizing of steel. Further investigations on the heterogeneous reactions leading to the

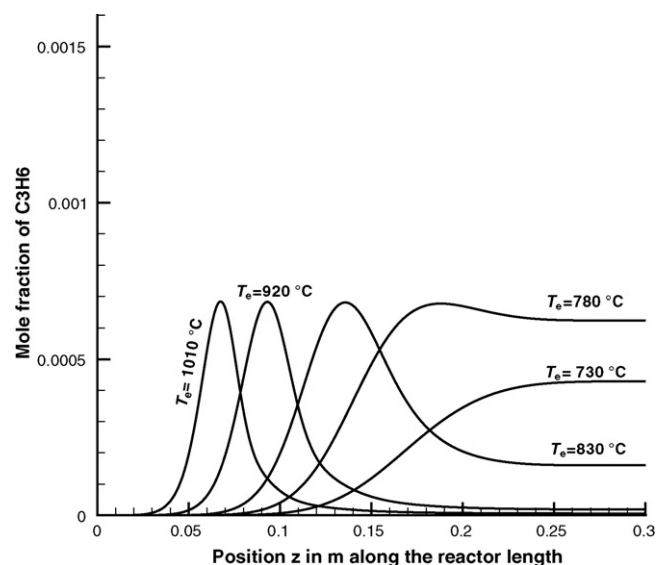


Fig. 16. C<sub>3</sub>H<sub>6</sub> mole fraction profiles for 1D model at different values of equivalent temperatures  $T_e$  (non-isothermal).

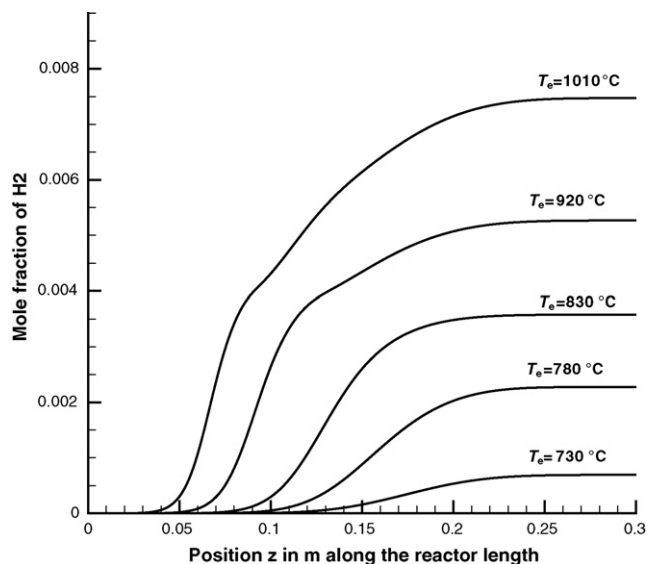


Fig. 17.  $H_2$  mole fraction profiles for 1D model at different values of equivalent temperatures  $T_e$  (non-isothermal).

carburizing of steel are required. The model developed in the present work needs to be extended by including such reactions so that it can be used to control the vacuum carburizing process.

## 6. Conclusion

Pyrolysis of propane has been studied under the particular technical operating conditions of vacuum carburizing of steel. The major species in the gas atmosphere have been identified and measured. Models using a detailed reaction mechanism with 1D and 2D flow field descriptions have been developed and used to simulate the reactor behavior. Comparison of experimental and simulation results is encouraging. The developed models can predict the carburizing gas compositions resulting from the homogeneous gas phase reactions of propane pyrolysis in the non-isothermal reactor over a range of temperatures with reference to the vacuum carburizing.

Modeling approach using detailed kinetics looks promising to advance the research in this field.

## References

- [1] K.M. Sundaram, G.F. Froment, *Chem. Eng. Sci.* 32 (1977) 601–608.
- [2] Z. Renjun, L. Qiangkun, L. Zhiyong, *J. Anal. Appl. Pyrol.* 13 (3) (1988) 183–190.
- [3] F. Billaud, *J. Anal. Appl. Pyrolysis* 21 (1/2) (1991) 15–25.
- [4] P. Dagaut, M. Cathonnet, J.C. Boettner, *Int. J. Chem. Kinet.* 24 (1992) 813–837.
- [5] E.N. Wami, *Chem. Eng. Technol.* 17 (1994) 195–200.
- [6] A.S. Tomlin, M.J. Pilling, J.H. Merkin, J. Brindley, N. Burgess, A. Gough, *Ind. Eng. Chem. Res.* 34 (11) (1995) 3749–3760.
- [7] L.T. Tel, *J. Anal. Appl. Pyrol.* 73 (2005) 231–247.
- [8] I. Ziegler, R. Fournet, P.M. Marquaire, *Appl. Pyrol.* 73 (2) (2005) 212–230.
- [9] C. Descamps, G.L. Vignoles, O. Féron, F. Langlais, J. Lavenac, *J. Electrochem. Soc.* 148 (10) (2001) 695–708.
- [10] K. Norinaga, O. Deutschmann, *Ind. Eng. Chem. Res.* 46 (11) (2007) 3547–3557.
- [11] F.S. Chen, K.L. Wang, *Surf. Coat. Technol.* 132 (1) (2000) 36–44.
- [12] L.D. Liu, F.S. Chen, *Mater. Chem. Phys.* 82 (2) (2003) 288–294.
- [13] L.D. Liu, F.S. Chen, *Surf. Coat. Technol.* 183 (2/3) (2004) 233–238.
- [14] F. Graf, S. Bajohr, R. Reimert, *Harerei-Technische Mitteilungen (Germany)* 58 (1) (2003) 20–23.
- [15] C.A. Trujillo, F. Graf, S. Bajohr, R. Reimert, *Chem. Eng. Technol.* 29 (3) (2006) 390–394.
- [16] J.S. Pierre, *Handbook, Heat Treating*, vol. 4, ASM International, 1991, pp. 348–351.
- [17] P. Jacquet, D.R. Rouse, G. Bernard, M. Lambertin, *Mater. Chem. Phys.* 77 (2) (2002) 542–551.
- [18] O. Deutschmann, S. Tischer, C. Correa, D. Chatterjee, S. Kleditzsch, V.M. Janardhanan, *Detchem Software Package, 2.0 ed.*, Karlsruhe, <http://www.detchem.com>, 2004.
- [19] H.D. Minh, PhD thesis, Faculty of Mathematics and Computer Science, University of Heidelberg, December 2005.
- [20] J. Warnatz, R.W. Dibble, U. Maas, *Combustion: Physical and Chemical Fundamentals, Modelling and Simulation, Experiments, Pollutant Formation*, Springer, 2001.
- [21] D.J. Hautman, R.J. Santoro, F.L. Dryer, I. Glassman, *Int. J. Chem. Kinet.* 13 (2) (1981) 149–172.
- [22] T. Koike, W.C. Gardiner Jr., *J. Phys. Chem.* 84 (16) (1980) 2005–2009.
- [23] S.K. Layokun, D.H. Slater, *Ind. Eng. Chem. Process Des. Dev.* 18 (2) (1979) 232–236.
- [24] C. Juste, G. Scacchi, M. Niclausa, *Int. J. Chem. Kinet.* 13 (9) (1981) 855–864.